Bull. Mater. Sci., Vol. 29, No. 7, December 2006, pp. 693–700. © Indian Academy of Sciences.

X-ray reflectivity investigation of interlayer at interfaces of multilayer structures: application to Mo/Si multilayers

M NAYAK*, G S LODHA and R V NANDEDKAR

Synchrotron Utilization Division, Centre for Advanced Technology, Indore 452 013, India

MS received 20 June 2006

Abstract. **We report the effect of interlayer on multilayer X-ray reflectivity (XRR) profile using simulations at 8·047 keV (CuK_α) energy. We distinguished the effect of interfacial roughness and in-depth interlayer on reflectivity profile. The interfacial roughness reduces the intensity of individual peak while the in-depth interlayer redistributed the reflectivity profile. We are able to discern the asymmetry in interlayer thickness at two interfaces if the interfacial roughness is small compared to in-depth interlayer thickness. The limitation is that, the sensitivity decreases with increasing interfacial roughness. This interlayer model is applied for electron beam evaporated Mo/Si multilayers. The Mo–on–Si interlayer thickness is 10 ± 0·5 Å and Si–on–Mo interlayer thickness is 8 ± 0·5 Å. The nature of interfacial compound is identified using X-ray photoelectron spectroscopy (XPS). The mechanism of interlayer asymmetry is explained on the basis of different heats of sublimation of Mo and Si.**

Keywords. **X-ray reflectivity; surfaces and interfaces; X-ray multilayer; X-ray photoelectron spectroscopy.**

1. Introduction

The X-ray reflectivity technique provides a non-destructive characterization of the internal interfaces of thin film multilayers (MLs). The specular X-ray reflectivity in glancing incident angle has been effectively utilized to characterize the interface morphology. XRR yields a density profile perpendicular to the sample surface (Parratt 1954) and modified (Nevot and Croce 1980) for real ML structures. Therefore, specular X-ray reflectivity gives information about the in-depth interlayer (i.e. interlayer thickness, density) present at the interfaces of ML structures. ML structures are used in a variety of fields, for e.g. X-ray optics (Spiller 1994). The main goal of a ML coating for the soft X-ray and extreme ultra-violet (EUV) region is to enhance reflectivity with moderate spectral resolution in regions of wavelengths and angles of incidence where single surfaces with useful reflectivity are not available. The efficiency of any optical devices, i.e. reflectance and resolution, is most sensitive to the coating parameter (Lodha *et al* 1994). Central to these issues are to understand the structure and growth of layers and interfaces. In view of optical performance of X-ray multilayer structures, especially density profile, including information on nature of interlayer (thickness, density), interfaces roughness and distribution of components, is crucial. Structural parameters of X-ray multilayers are mostly obtained using X-ray reflectivity, X-ray diffuse scattering and cross-sectional transmission electron microscopy (Barbee *et al* 1985; Lodha *et al* 1996; Freitag and Clemens 2001; Lim *et al* 2001). The systematic simulation of effect of nature of interlayer (interlayer thicknesses, stoichiometry) on specular XRR and comparison with experimental data is lacking. Some authors only report the XRR fitted using three and four-layer models (Kim *et al* 1988; Slaughter *et al* 1994). Here, we report systematic studies of the effect of interlayer on Mo/Si MLs using simulation of XRR and compare with experimental results.

Mo/Si MLs are efficient mirrors (Barbee *et al* 1985; Hoover *et al* 1991; Toyoda *et al* 2000) in the soft X-ray region (130–300 Å) due to high reflectivity and used in technological applications such as lithography, astronomy, X-ray microscopy and spectroscopy. The interface quality plays a decisive role in achieving an optimum performance of MLs for X-ray optics. Again the Mo/Si MLs are attracted to superconductor community due to their superconducting properties (Nakajima *et al* 1989). They suggested that the superconducting properties of Mo/Si MLs conformed to results from amorphous MoSi phase formed in the interfacial region of the sub-layers. Therefore, the nature of interfaces (i.e. interlayer thickness, phase and stoichiometry) in Mo/Si MLs is of considerable practical interest. According to previously available results, Si–on–Mo interface is thinner than Mo–on–Si and the interlayer is a mixture of Mo and Si observed using TEM (Petford-long *et al* 1987; Stearns *et al* 1992; Ulyanenkov 2000). On the other hand, by using the same technique, it has been observed that amorphous interlayer silicide is found at the

*Author for correspondence (mnayak@cat.ernet.in)

Mo–on–Si interface but not at the Si–on–Mo interface (Slaughter *et al* 1990). The nature of the interlayer (phase and stoichiometry) obtained using TEM may be erroneous if the interface compound is amorphous and very thin, ~1 nm (Bravman and Sinclair 1984). The observation of small asymmetry (~2 Å) at two interfaces using TEM may be difficult due to poor image contrast between interlayer and pure elements. Some authors have also used XRR method using trilayer model (Slaughter *et al* 1994) and four-layer model (Kim *et al* 1988) to fit experimental data without detailed studies on the effect of nature of interlayer on reflectivity profile and the effect or roughness on small interlayer asymmetry value. Using four-layer model, Kim *et al* (1988) reported small asymmetry of 2·6 Å (Mo–on–Si interlayer, 4·6 Å and Si–on–Mo, 2 Å) when the roughness was 6 Å (greater than the interlayer width). This seems to be unphysical as the interlayer thickness is smaller than interface roughness. To the best of our knowledge, the effect of nature of interlayer on specular X-ray reflectivity profile and comparison with measured data are not reported.

In this article, we have shown the distinct difference between effect of interfacial roughness and in-depth subnanometer interlayer on X-ray reflectivity profile. We have been able to determine the atomic scale asymmetry of interlayer thickness at the interfaces and its sensitivity with respect to interfacial roughness. We have extracted quantitative information on the nature of interlayer present in the MLs. The phase of interlayer compound is identified using XPS. The experimental results are discussed with respect to XRR simulations. The possible mechanism of asymmetry is suggested.

2. Experimental

Mo/Si MLs were deposited using an ultra high vacuum electron beam evaporation system (base pressure, ~2×10^{-9} mbar). The substrates used were super polished Si(111) wafers with surface rms roughness, ~4 Å, measured by XRR before deposition of MLs. The thickness was measured using quartz crystal coupled to programmable frequency counter (model HM 8122). The MLs were fabricated with a number of layer pairs ranging from 4–20, with a modulation period, 100 Å. The Γ-ratio, which is the ratio of Mo thickness to the period thickness in the period was kept constant at Γ = 0·29. The top layer was silicon. The deposition rate was kept at ~1 Å/min. XRR measurements were carried out on a reflectometer (Suresh *et al* 2000) equipped with a sealed Cu tube as source of X-rays. The X-ray source was operated at 40 kV and 30 mA. The XPS measurements were carried out using a photoelectron spectrometer equipped with an OMICRON electron analyser (model EA 125). X-ray source used was Al K_α. Argon ion etching gun was used for depth profiling of the MLs.

3. Results

3.1 *Hard X-ray reflectivity*

The typical angle dependent reflectivity spectra of Mo/Si MLs for N = 4, 10 and 20 are shown in figure 1. The experimental data are simulated by two-layer model (Parratt 1954) and taking roughness for real ML structures (Nevot and Croce 1980). The ML structures show Bragg peak up to 5th order with distinct Kiessig oscillations between the successive Bragg peaks (clearly visible for ML with smaller number of layer pairs) indicating good quality of multilayer structures. Figure 1 shows the comparison of the intensities of the Bragg peaks between experimental data and simulation, taking into account the reduction of the intensities due to interfacial roughness in statistical approach (two-layer model). The difference between experimental and simulation results indicate the presence of interlayer due to inter-diffusion at the interfaces in Mo/Si MLs.

In the subsequent sections, we demonstrate the effect of interlayer and its asymmetry on the reflectivity profile using simulations by incorporating interlayer in Parratt's formalism.

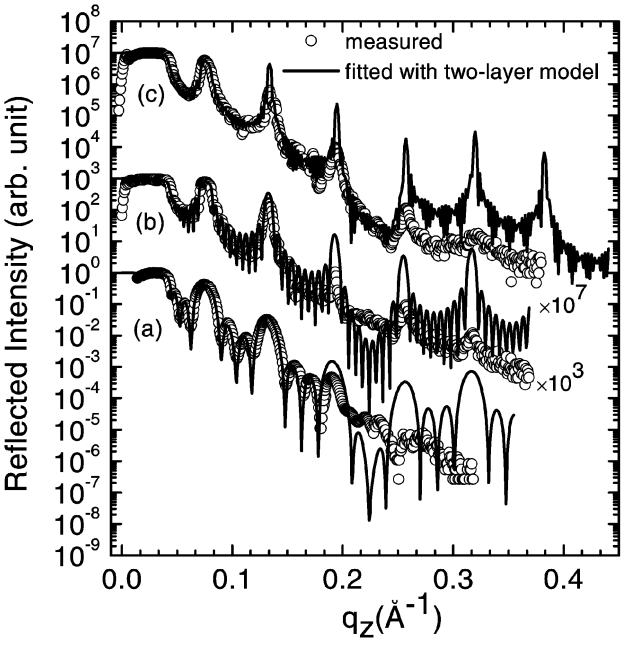

Figure 1. XRR spectra of Mo/Si multilayers with modulation period, 100 Å and Γ = 0·29 measured at 8·047 keV energy. (a) For multilayer with a number of layer pairs, N = 4, (b) for multilayer with N = 10, (c) for multilayer with N = 20. Open circles represent the measured data. The continuous line shows calculated spectra assuming two-layer model. For N = 4, roughness of Si and Mo are 4 and 5 Å, respectively. For N = 20, roughness of Si and Mo are 10 and 11 Å, respectively.

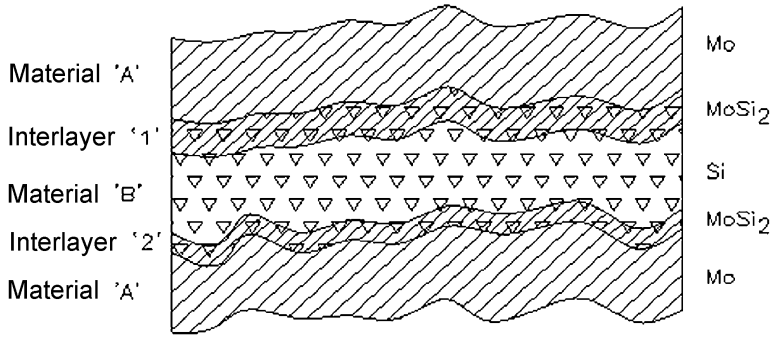

Figure 2. A schematic diagram of real multilayer structure with interlayer. The four-layer model shows imperfect boundaries and interlayer in between two pure Mo and Si layers.

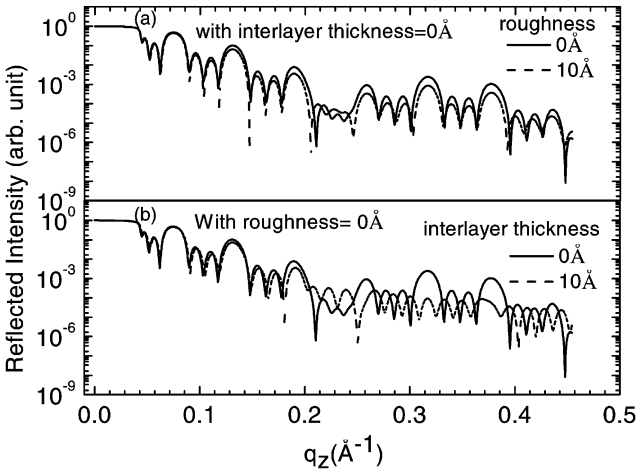

Figure 3. The simulated spectra of Mo/Si ML for a number of layer pairs, $N = 4$ with periodicity, 100 Å and $\Gamma = 0{\cdot}29$ at 8·047 keV energy. (a) Effect of roughness on reflectivity profile with zero interlayer thickness. As the roughness increases, the intensity of whole reflectivity profile decreases and its effect is more at higher order Bragg peaks and (b) effect of interlayer on reflectivity profile with zero roughness. As interlayer thickness increases, the whole reflectivity profile redistributed.

3.1.1 *Modeling and simulation*

The interfaces of any real ML system are imperfect due to roughness, interdiffusion and chemical reactivity of materials. The imperfect interfaces can be dealt either by statistical approach (two-layer model) or multiple layer models with the incorporation of interlayer between two layer systems. In the statistical approach, the reflectance from a multilayer structure with N layers can be calculated using recursion formalism (Parratt 1954). For an ideal ML with sharp interfaces the composition is defined by a Γ-ratio. But when a compound material is formed at the interface, the interlayer model gives a better fitting to the reflected profile than the statistical approach. The interlayer is due to inter-diffusion at the imperfect boundaries.

Figure 2 shows a four-layer model, which incorporates the interlayer in between pure materials of Si and Mo. Note that the period of ML is $d = d_1 + d_{12} + d_{21} + d_2$. The thickness of the interlayers, d_{12} and d_{21}, may not be the same, and such a structure cannot be described by the Γ-ratio used in the statistical approach. The effective Γ-ratio (Yakshin *et al* 2002) to take into account the formation of interlayer with thicknesses, d_{12} and d_{21}, and corresponding refractive indices, δ_{12} and δ_{21}, is

$$\Gamma_{\text{eff}} = \frac{d_1 + (d_{12}w_{12} + d_{21}w_{21})}{d}, \tag{1}$$

where the weight factor, w, for compounds at different boundaries is defined as

$$w_{12} = \left|\frac{\delta_{12} - \delta_2}{\delta_1 - \delta_2}\right|, \quad w_{21} = \left|\frac{\delta_{21} - \delta_2}{\delta_1 - \delta_2}\right|, \tag{2}$$

δ_1 and δ_2 are the refractive indices of the high-Z and low-Z materials, respectively. In the case of Mo/Si MLs, the four layers consist of Mo and Si layers and two interlayers of silicide. The structure of the coating can be written as $[Si/Mo_{x1}Si_{y1}/Mo/Mo_{x2}Si_{y2}]_N + Si + SiO_2$. Here N is the number of periods and last two layers correspond to a partially oxidized top layer of Si. The interlayer which takes into account the formation of a compound, is taken as $MoSi_2$ from our XPS measurements.

3.1.1a *Influence of interlayer:* The significant influence of interlayer on the reflectivity profile, compared with statistical interface roughness is shown in figure 3. We have simulated at 8·047 keV energy and compared with experimental results. We have taken a small number of layer pairs of Mo/Si ML coated on silicon substrate to show the clear influence on Kiessig oscillations on full reflectivity profile. Figure 3(a) shows the effect of interface roughness on reflectivity profile assuming zero interlayer thickness (two-layer model). As the interface roughness increases the reflectivity reduces without affecting

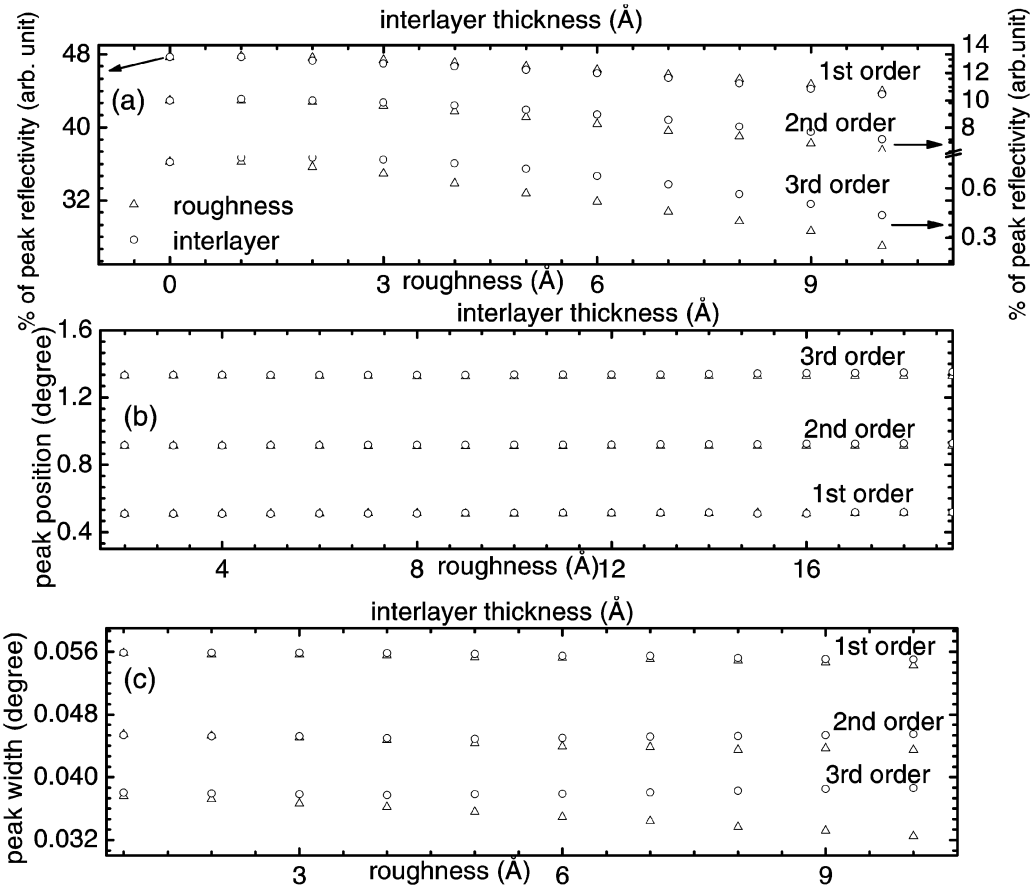

Figure 4. The simulation studies of the effect of roughness (open triangles) and interlayer (open circles) on higher order Bragg's peak for $N = 4$ MLs. (a) Effect on higher order Bragg peak reflectivity, (b) effect on higher order Bragg peak position and (c) effect on higher order Bragg peak width.

the distribution of individual peak. Figure 3(b) shows the zero interface roughness and the effect of interlayer thickness on reflectivity profile. As the interlayer thickness increases, the reflectivity of Bragg peaks decreases as well as the peak position shifts due to change in refraction correction term. The figure also indicates the higher order Bragg peaks where intensity reduces more with increasing interlayer thickness as compared to interface roughness. This is because of a decrease in refractive index in contrast to formation of interlayer. It is to be noted here that the interlayer leads to redistribution of reflectivity curve, which is not the case when no interlayer is present. Therefore, figure 3 provides clear information about the difference in effect of interfacial roughness and in-depth sub-nanometer interlayer on reflectivity profile. A comparison of simulation study of the effect of roughness and interlayer on higher order Bragg peak reflectivity, peak position and peak width is shown in figure 4. It is clear that the effect of interlayer is significantly compared to roughness on higher order Bragg peak reflectivity, peak position and peak width. This is because the higher order Bragg peaks appear at higher q_z values.

3.1.1b *Effect of asymmetry:* An intrinsic property of as deposited Mo/Si ML is that, the formation of interlayer viz. Mo–on–Si and Si–on–Mo, is asymmetric. Figure 5 shows the effect of atomic scale asymmetry in interlayer thickness for different roughness values. Figure 5(a) shows that the small in-depth interlayer thickness asymmetry (~2 Å) is clearly identified in MLs with small roughness. The effect is more at larger q_z value. Again as interfacial roughness increases (as can be seen in figures 5(a)–(c)), the sensitivity of interlayer asymmetry decreases. We have observed an ambiguity in the asymmetry of interlayer for ML if interfacial roughness is comparable to the interlayer thickness as shown in figure 5(c). In this case, our simulation values give almost the same results as when the two interlayer thicknesses are exchanged. This also has been observed experimentally and is discussed in §4.

3.1.1c *Application to Mo/Si multilayer:* We have simulated for all possible stoichiometric combinations for Mo and Si at the interfaces. The best result indicates that at the interface Mo : Si ratio is 1 : 2. Figure 6 shows the experimental data fitted with incorporation of interlayer.

This model results in best fits up to all the higher order Bragg peaks indicating real structure in the ML stacks. The inset of figure 6 clearly shows the distinct Kiessig oscillations up to 1st Bragg peak which indicates well-defined multilayer structure with good control over deposited thicknesses. The decrease in intensity of the higher order peaks, compared to a two-layer model, arises because of poor refractive index contrast at the interfaces due to formation of interlayer. The quantitative numbers for individual layer thickness, interface roughness, interlayer thickness and optical constant deduced from best fit is tabulated in table 1. The measured thickness values of the Si and Mo layers are expected to be smaller than the nominal value, since the measurement includes formation of interlayer at the interfaces due to inter mixing of Mo and Si during deposition. The Mo–on–Si interlayer thickness is 10 ± 0·5 Å whereas Si–on–Mo interlayer thickness is 8 ± 0·5 Å. In figure 7(a), the scattering length density is plotted as a function of depth of ML for $N = 4$, as obtained from fitting of experimental data. The distance between centre of two successive maxima (pure Mo) or two successive minima (pure Si) corresponds to period of ML. In figure 7(b), dashed line (----) corresponds to the observed interface region arising due to the combination of silicide interlayers and layer roughness, whereas the dotted line (.....) represents the calculated profile without the Gaussian roughness. The interlayer regions as marked in figure 7(b) on two sides are asymmetric. Also figure 7(b) indicates the presence of native oxide (~10 Å) at the top of MLs.

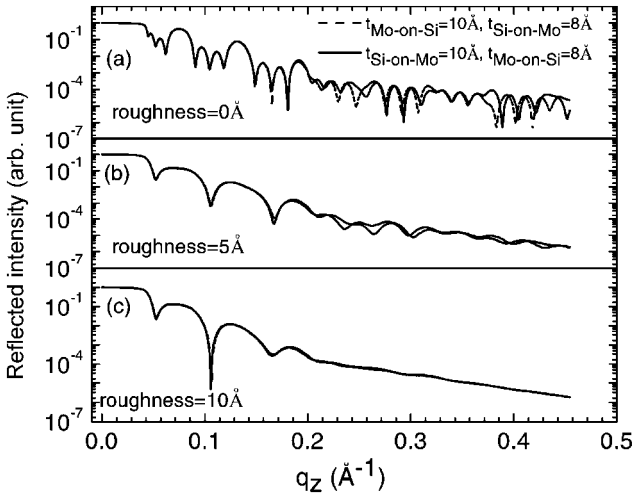

Figure 5. The simulation spectra of the effect of asymmetry interlayer thickness on reflectivity profile of $N = 4$ MLs for different roughness values.

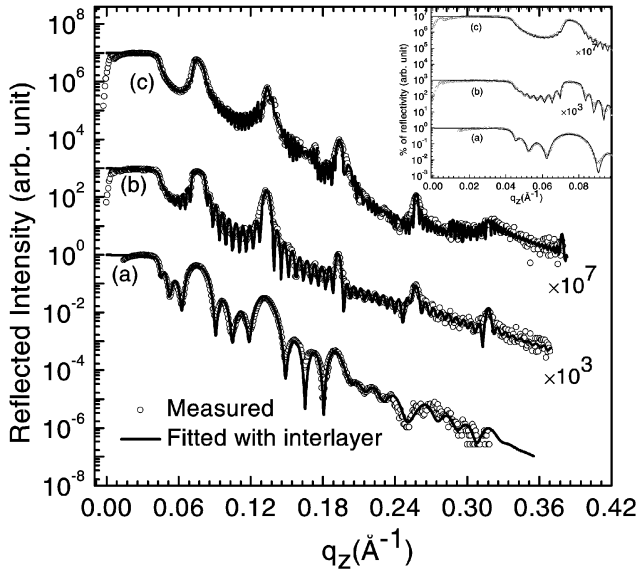

Figure 6. The Mo/Si MLs measured reflectivity data of figure 1 is re-plotted along with four-layer model fitting. Open circles represent the measured data. The continuous line shows calculated spectra with four-layer model: (a) for MLs with $N = 4$, (b) for MLs with $N = 10$ and (c) for MLs with $N = 20$. The inset shows the distinct Kiessig oscillations up to 1st Bragg peak.

3.2 *X-ray photoelectron spectroscopy*

The Mo 3*d* core level spectra of pure Mo and Mo located at the interface region of Mo/Si systems are shown in

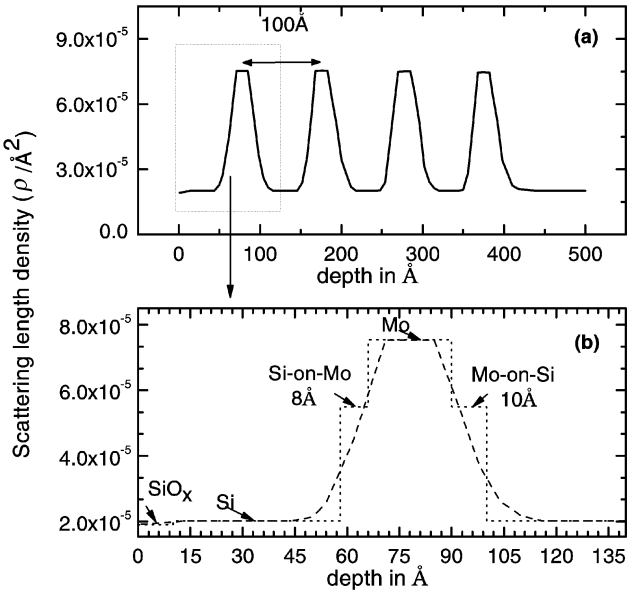

Figure 7. Scattering length density profile obtained after fitting of experimental data using interlayer. (a) Maxima and minima correspond to layers of pure Mo and Si, respectively. In between are the interface region arising from the formation of silicide interlayer and layer roughness and (b) the dashed (-----) line represents actual profile used for fitting assuming interlayers with Gaussian roughness. The dotted (.....) line represents the profile without Gaussian roughness.

Table 1. The best fit XRR experimental results fitted with four-layer model for Mo/Si MLs.

No. of layer pairs	Layer	Thickness (Å)	Roughness (Å)	Indices ($\times 10^{-6}$)	Absorption* ($\times 10^{-6}$)
4	Si	58 ± 0·5	4	6·3 [7·59]	0·15 [0·173]
	Si–on–Mo	8 ± 0·5	4	19·3 [20·944]	1·18 [1·248]
	Mo	24 ± 0·5	5	28·3 [28·8]	1·4 [1·88]
	Mo–on–Si	10 ± 0·5	4	19·3 [20·944]	1·18 [1·248]
10	Si	58 ± 0·5	7	6·3 [7·59]	0·15 [0·173]
	Si–on–Mo	8 ± 0·5	7	19·3 [20·944]	1·18 [1·248]
	Mo	24 ± 0·5	8	28·3 [28·8]	1·4 [1·88]
	Mo–on–Si	10 ± 0·5	7	19·3 [20·944]	1·18 [1·248]
20	Si	58 ± 0·5	10	6·3 [7·59]	0·15 [0·173]
	Si–on–Mo	8 ± 0·5	10	19·3 [20·944]	1·18 [1·248]
	Mo	24 ± 0·5	11	28·3 [28·8]	1·4 [1·88]
	Mo–on–Si	10 ± 0·5	10	19·3 [20·944]	1·18 [1·248]

*In square bracket the tabulated values of optical constants (indices and absorption) from Henke *et al* (1993).

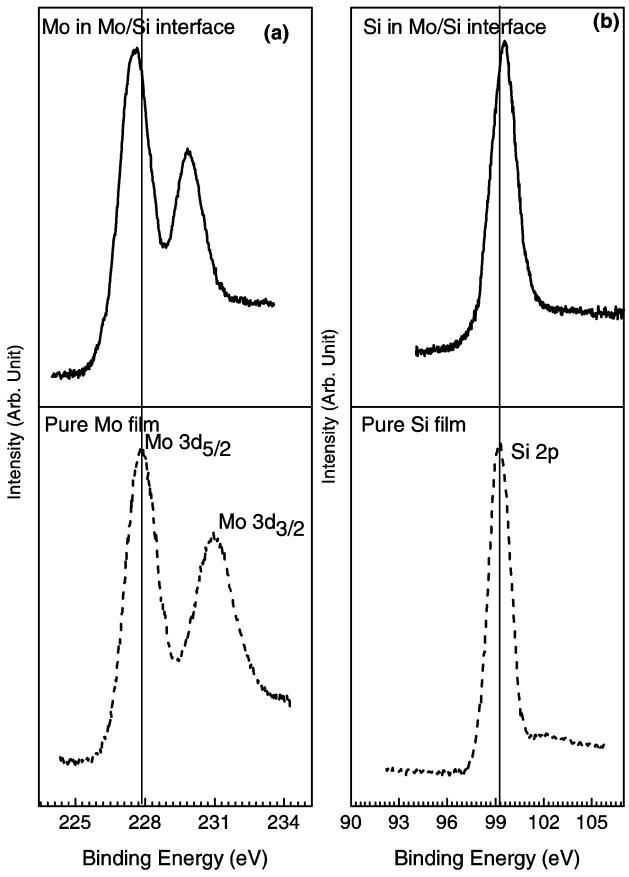

Figure 8. XPS spectra using Al K_α source. (a) Mo 3*d* core level spectra recorded for pure Mo film (dash) and Mo at interfaces of Mo/Si MLs and (b) Si 2*p* core level spectra recorded for pure Si film (dash) and Si at interfaces of Mo/Si MLs.

figure 8(a). In pure Mo film, Mo $3d_{5/2}$ and $3d_{3/2}$ lines appear at 227·9 and 231·02 eV, respectively. At the interface region, Mo $3d_{5/2}$ and $3d_{3/2}$ lines appear at 227·5 and 230·61 eV, respectively. Although the shape of line of the spectra is similar, a shift of 0·4 eV is observed to lower binding energy side for the curve recoded at the interface. Similarly, the Si 2*p* core level spectra of pure Si and Si located at the interface region of Mo/Si systems are shown in figure 8(b). In pure Si film, Si 2*p* line appears at 99·19 eV whereas at interface region Si 2*p* line appears at 99·39 eV. In this case, Si 2*p* line shifts by 0·2 eV to higher binding energy side for curve recorded at interface.

4. Discussion

Table 1 shows that the Si–on–Mo interlayer thickness is 8 ± 0·5 Å whereas Mo–on–Si is 10 ± 0·5 Å. The error may be due to the uncertainty in the estimation of the weight factor, ω, for the composition of compound at the boundaries. It is important to indicate that, Mo–on–Si interlayer thickness is higher than Si–on–Mo interlayer and is clearly observed for $N = 4$ and $N = 10$ layer pair MLs in figures 6(a) and (b), but for $N = 20$ layer pair MLs in figure 6(c), we have observed an ambiguity in the asymmetry of interlayer because our experimentally fitted values give almost the same results when the two interlayer values are exchanged. This is because for $N = 20$ layer pair sample interfacial roughness is comparable to in-depth interlayer thickness as shown in table 1. Therefore, when the roughness is comparable to interlayer thickness, roughness effect dominates and it becomes difficult to observe the small asymmetry (~2 Å) in the interlayer. This also agrees with our simulation results shown in figure 5. Using four-layer model, Kim *et al* (1988) reported that Mo–on–Si interlayer thickness is 4·6 Å whereas that of Si–on–Mo is 2 Å (asymmetry 2·6 Å) with roughness, 6 Å (greater than interlayer thickness). As per their best-fit XRR figure, the fitted data do not reflect the real structure in their MLs. In their XRR fitting, the authors might have used interlayer thickness value from their TEM results without any detailed fitting. Hence, we conclude that small asymmetry (~2 Å) in interlayer thickness will be able to discern using specular XRR, when the roughness is small as comparable with the interlayer

thickness that we observed theoretically and experimentally. Our value of interlayer thickness agrees well with that observed previously (Bajit *et al* 2001). However, our results of interlayer thickness differ significantly with those observed by TEM and XPS (Petford-long *et al* 1987; Stearns *et al* 1990; Jdiyaou *et al* 1992). This may be due to use of different characterization techniques. In TEM, the error in small atomic scale asymmetry of interlayer thickness may be due to poor image contrast between interlayer and pure elements. Whereas in XPS, the error in interlayer asymmetry is due to poor thickness resolution during depth profiling. We have extracted interlayer composition in the mixture of Mo : Si as 1 : 2 from optical constant of best-fit XRR data. To conform stoichiometry of interlayer, we have observed interlayer phase and stoichiometry from XPS measurements. From figure 8, a shift of –0·4 eV of Mo 3*d* line for curve recorded at interface and a shift of +0·2 eV of Si 2*p* line for curve recorded at interface reveals formation of $MoSi_2$ phase at the interface (Slaughter *et al* 1991). We have done detailed investigation of Mo/Si interface using XPS which will be reported elsewhere. Therefore, the composition extracted from XRR best-fit data well agrees with XPS results. In table 1, the value of optical constants (indices and absorption) for Si, Mo and $MoSi_2$ interlayer obtained from XRR best fit are slightly different from tabulated value in square bracket from Henke *et al* (1993), and is attributed to density change.

Different authors suggest the possible mechanism of asymmetry in as deposited Mo/Si MLs. Some authors (Petford-long *et al* 1987; Ulyanenkov *et al* 2000; Bajit *et al* 2001) proposed kinetic model (different momentum of Si and Mo) in the role of formation of interlayer during deposition in Mo/Si multilayers. Some authors (Windt *et al* 1992) proposed the initial formation of amorphous interlayer due to Si diffusion processes, in which the Si atoms tend to migrate, as the Mo atoms are deposited, while some authors (Slaughter *et al* 1994) estimated the activation energy using Arrhenius analysis of the variation of silicide thickness from TEM data. From estimated activation energy, they suggested a surface diffusion process rather than bulk diffusion process. On the other hand, it has been suggested that (Stearns *et al* 1990) Mo atoms get easily embedded into relatively open and disorder amorphous Si than Si into more closely packed crystalline Mo lattice. The same authors (Stearns *et al* 1992) observed that interlayer thickness variation with temperature is consistent with a process that is atleast partly thermally activated. It has also been proposed (Liwen *et al* 1997) that the asymmetry in sputtered deposited Mo/Si MLs is due to thermally activated processes by considering different thermal conductivities of Si and Mo. Also it has been tried (Morgan and Boercker 1991) to explain the mechanism of asymmetry using molecular beam dynamics study. They suggested that different degrees of penetration and interdiffusion of the adatoms during deposition is the cause of asymmetry. If the kinetic model plays a role in the formation of interlayer at the interfaces, then evaporated MLs would not show interlayers. This is because, the energies of evaporated and sputtered atoms are ~0·2 eV and ~10 eV, respectively (Petford-long *et al* 1987; Stearns *et al* 1992), whereas the cohesion energies of amorphous Si and Mo are ~3 eV and ~7 eV (Kittel 1976), respectively, which are greater than energy of the evaporated atom. Interlayer in as deposited Mo/Si MLs is independent of deposition process. Therefore, we feel the kinetic model would not play a role in formation of interlayer in as deposited Mo/Si multilayers. Silicon is the predominant diffusant in Mo–Si binary system (Murarka 1983). In the Mo/Si system, an intensive atomic intermixing takes place at the boundary during deposition because of a low activation energy of surface diffusion for Si (Stearns *et al* 1992) (~0·2 eV) and local temperature effect. The asymmetry in the interlayer is due to difference in heat of sublimation of Mo and Si. This affects diffusion of Si in Si–on–Mo and Mo–on–Si cases differently. The initial intermixing would be a thermally activated process by the negative thermodynamic heat of mixing, because any process involving condensation from the vapour will release latent heat. The latent heat of sublimation (Brandes and Brook 1992) of Mo and Si is 664·5 and 450·1 KJ g-atom^{-1}, respectively. The thermal conductivity of Mo is higher than Si. So, the heat produced on the Si surface by the Mo adatoms will be large and diffuse slowly due to lower thermal conductivity compared to that of Si deposition on Mo surface. This may lead to a higher local temperature in Mo–on–Si case and hence more probability of surface diffusion for silicon. When the interlayer thickness reaches $10 \pm 0{\cdot}5$ Å, it becomes a barrier for further surface diffusion of Si. Similarly in Si–on–Mo case, the local rise in temperature may be lower. Since Si is the dominant diffusant in Mo/Si system, therefore, after arrival of Si on Mo surface, Si has to diffuse through bulk diffusion in the Mo layer. Since the coefficient of bulk diffusion for Si is very low in low temperature range (Yulin *et al* 2002) and local rise in temperature is low, so, there is less probability of bulk diffusion and hence a thin interlayer of thickness, $8 \pm 0{\cdot}5$ Å, is formed at Si–on–Mo interfaces. When the interlayer thickness reaches $8 \pm 0{\cdot}5$ Å, it becomes a barrier for further bulk diffusion of Si. Therefore, interlayer thickness is independent of number of layer pairs as given in table 1. Therefore, at the interface region the supply of metal atom is limited due to thermal effects that favour the transport of Si atoms over Mo atoms which in turn energetically favoured Si-rich stoichiometry (Murarka 1983) as we observed using XPS.

5. Conclusions

We have demonstrated presence of interlayer at the interfaces of Si-based multilayer structures using XRR inves-

tigation. A detailed simulation study has been done on the effect of in-depth interlayer thickness and its asymmetry on reflectivity profile. The interlayer, which takes into account the formation of compound in the interface, causes the redistribution of reflectivity patterns whereas the roughness parameters reduce the reflected intensity. For multilayer with small roughness, the small interlayer asymmetry (~2 Å) is clearly discernible. This model is applied for e-beam evaporated Mo/Si multilayers. The best-fit data reveal that the interlayer is asymmetric. The Mo–on–Si interlayer thickness is $10 \pm 0{\cdot}5$ Å whereas Si–on–Mo interlayer thickness is $8 \pm 0{\cdot}5$ Å. XPS measurement indicates formation of $MoSi_2$ phase at the interfaces. The mechanism of asymmetry is due to different heats of sublimation of Mo and Si.

Acknowledgements

We would like to thank Ajay Gupta and Amit Sarayia for help in XRR measurements, S M Chaudhari for XPS measurements and M H Modi for useful discussion.

References

Bajit S, Stearns D G and Kearney P A 2001 *J. Appl. Phys.* **90** 1017

Barbee T W, Mrowka Jr S and Hettrick M C 1985 *Appl. Opt.* **24** 883

Brandes E A and Brook G B (eds) 1992 *Smithells metals reference book* (Jordan Hill, Oxford, London: Butterworth-Heinemann) 7th ed., p. 82

Bravman J C and Sinclair R 1984 *J. Electron Microsc. Technol.* **1** 53

Freitag J M and Clemens B M 2001 *J. Appl. Phys.* **89** 1101

Henke B L, Gullikson E M and Davis J C 1993 *Atomic data and nuclear data table* **54** 181

Hoover R B, Shealy D L, Brinkley B R, Backer P C, Barbee T W and Walker A B C 1991 *Opt. Engg.* **30** 1086

Jdiyaou Y I, Azizan M, Ameziane E L, Brunel M and Nguyen T A 1992 *Appl. Surf. Sci.* **55** 165

Kim D E, Lee S M, Jeon I J and Yanagihara M 1988 *Appl. Surf. Sci.* **127–129** 531

Kittel C 1976 *Introduction to solid state physics* (New York: Wiley)

Lim Y C, Westerwalbesloh T, Aschentrup A, Wehmeyer O, Haindl G, Kleineberg U and Heinzmann U 2001 *Appl. Phys.* **A72** 121

Liwen W, Wei S, Wang B and Liu W 1997 *J. Phys.: Condens. Matter* **9** 3521

Lodha G S, Yamashita K, Suzuki T, Hatsukade I, Tamura K, Ishigami T, Takahama S and Namba Y 1994 *Appl. Opt.* **33** 5869

Lodha G S, Pandita S, Gupta A, Nandedkar R V and Yamashita K 1996 *Appl. Phys.* **A62** 29

Morgan W L and Boercker D B 1991 *Appl. Phys. Lett.* **59** 1176

Murarka S P 1983 *Silicides for VLSI applications* (Orlando: Academic)

Nakajima H, Ikebe M, Muto Y and Fujimori H 1989 *J. Appl. Phys.* **65** 1637

Nevot L and Croce P 1980 *Rev. Phys. Appl.* **15** 761

Parratt L G 1954 *Phys. Rev.* **95** 359

Petford-long A K, Stearns M B, Chang C-H, Nutt S R, Stearns D G, Ceglio N M and Hawryluk A M 1987 *J. Appl. Phys.* **61** 1422

Slaughter J M, Kearney P A, Schulze D W and Falco C M 1990 *Proc. SPIE* **1343** 73

Slaughter J M *et al* 1994 *J. Appl. Phys.* **76** 2144

Slaughter J M, Shapiro A, Kearney P A and Falco C M 1991 *Phys. Rev.* **B44** 3854

Spiller E 1994 *Soft X-ray optics* (Washington: SPIE-The International Society for Optical Engineering)

Stearns D G, Stearns M B, Chang Y, Stith J H and Ceglio N M 1990 *J. Appl. Phys.* **67** 2415

Stearns M B, Chang C H and Stearns D G 1992 *J. Appl. Phys.* **71** 187

Suresh N, Modi M H, Tripathi P, Lodha G S, Chaudhri S M, Gupta A and Nandedkar R V 2000 *Thin Solid Films* **368** 80

Toyoda M, Shitami Y, Yanagihara M, Ejima T, Yamamoto M and Watanabe M 2000 *Jpn J. Appl. Phys.* **39** 1926

Ulyanenkov A, Matsuo R, Omote K, Inaba K and Harada J 2000 *J. Appl. Phys.* **87** 7255

Windt D L, Hull R and Waskiewicz W K 1992 *J. Appl. Phys.* **71** 2675

Yakshin A E, Louis E, Gorts P C, Maas E L G and Bijkerk F 2002 *Physica* **B283** 143

Yulin S *et al* 2002 *J. Appl. Phys.* **92** 1216